



UNIVERSITY OF LEEDS

This is a repository copy of *Probing Mechanical Properties of Water-Crude Oil Interfaces and Colloidal Interactions of Petroleum Emulsions using Atomic Force Microscopy*.

White Rose Research Online URL for this paper:
<http://eprints.whiterose.ac.uk/113236/>

Version: Accepted Version

Article:

Kuznicki, NP, Harbottle, D, Masliyah, JH et al. (1 more author) (2017) Probing Mechanical Properties of Water-Crude Oil Interfaces and Colloidal Interactions of Petroleum Emulsions using Atomic Force Microscopy. *Energy & Fuels*, 31 (4). pp. 3445-3453. ISSN 0887-0624

<https://doi.org/10.1021/acs.energyfuels.6b02451>

© 2017 American Chemical Society. This document is the Accepted Manuscript version of a Published Work that appeared in final form in *Energy & Fuels*, copyright © American Chemical Society after peer review and technical editing by the publisher. To access the final edited and published work see <https://doi.org/10.1021/acs.energyfuels.6b02451>.
Uploaded in accordance with the publisher's self-archiving policy.

Reuse

Unless indicated otherwise, fulltext items are protected by copyright with all rights reserved. The copyright exception in section 29 of the Copyright, Designs and Patents Act 1988 allows the making of a single copy solely for the purpose of non-commercial research or private study within the limits of fair dealing. The publisher or other rights-holder may allow further reproduction and re-use of this version - refer to the White Rose Research Online record for this item. Where records identify the publisher as the copyright holder, users can verify any specific terms of use on the publisher's website.

Takedown

If you consider content in White Rose Research Online to be in breach of UK law, please notify us by emailing eprints@whiterose.ac.uk including the URL of the record and the reason for the withdrawal request.



eprints@whiterose.ac.uk
<https://eprints.whiterose.ac.uk/>

Probing Mechanical Properties of Water-Crude Oil Interfaces and Colloidal Interactions of Petroleum Emulsions using Atomic Force Microscopy

Natalie P. Kuznicki,[†] David Harbottle,^{†‡} Jacob H. Masliyah,[†] Zhenghe Xu^{†*}

[†] Department of Chemical and Materials Engineering, University of Alberta, Edmonton, Canada

[‡] School of Chemical and Process Engineering, University of Leeds, Leeds, UK

ABSTRACT

Atomic force microscopy (AFM) is frequently used to elucidate complex interactions in emulsion systems. However, comparing results obtained with “model” planar surfaces to curved emulsion interfaces often proves unreliable, since droplet curvature can affect adsorption and arrangement of surface-active species, while droplet deformation affects the net interaction force. In the current study, AFM was utilized to study the interactions between a colloidal probe and water droplet. Force magnitude and water droplet deformation were measured in asphaltene and bitumen solutions of different concentrations at various droplet aging times. Interfacial stiffening and an increase in particle-droplet adhesion force were observed upon droplet aging in bitumen solution. As reported in our previous study (Kuznicki, N. P.; Harbottle, D.; Masliyah, J.; Xu, Z. Dynamic Interactions between a Silica Sphere and Deformable Interfaces in Organic Solvents Studied by Atomic Force Microscopy. *Langmuir* 2016, 32 (38), 9797–9806), a viscoelasticity parameter should be included in the high force Stokes-Reynolds-Young-Laplace (SRYL) equations to account for the interfacial stiffening and non-Laplacian response of the water droplet at longer aging times. However, following the addition of a biodegradable demulsifier, ethyl cellulose (EC), an immediate reduction in both the particle-droplet adhesion force and the rigidity of the water droplet occurred. Following EC addition, the interface reverted back to a

Laplacian response and droplet deformation was once again accurately predicted by the classical SRYL model. These changes in both droplet deformation and particle-droplet adhesion, tracked by AFM, imply a rapid asphaltene/bitumen film displacement by EC molecules. The colloidal probe technique provides a convenient way to quantify forces at deformable oil/water interfaces and characterize the in-situ effectiveness of competing surface active species.

INTRODUCTION

Stable water-in-crude oil emulsions pose a challenge in the petroleum industry. Small water droplets and solids, a few microns in diameter, cannot be completely removed during surface processing and thus migrate downstream, accelerating corrosion and equipment malfunctions which can lead to production losses.¹⁻³ These fine water droplets are stabilized by a layer of hydrocarbons and do not coalesce, even under applied load. The main hydrocarbon fraction responsible for the high emulsion stability is believed to be asphaltenes, the most problematic surface-active component in crude oils.⁴ Asphaltenes are defined as a fraction of crude oil which is soluble in toluene and insoluble in n-heptane.¹ Steric stabilization from the interfacial asphaltene layers and non-uniform drainage of the intervening liquid films, as water droplets are pressed together, lead to enhanced emulsion stability.⁵⁻⁷ The strongly elastic interfacial layers act as a mechanical barrier between water droplets and must be deformed beyond the shear yield strength to initiate droplet coalescence.^{4,5,7,8} Although other bitumen components such as resins and naphthenic acids cannot stabilize water-in-oil emulsions alone, they interact with asphaltenes to enhance emulsion stability.^{9,10} Asphaltenes are also known to change the surface properties of hydrophilic solids (clays), making them bi-wettable and enhancing their potential to partition at the oil-water interface.¹¹⁻¹³ Solids of intermediate hydrophobicity (water contact angles close to

90°) and in the size range of 0.22 - 8 μm were shown to most effectively stabilize water-in-oil emulsions.¹⁴

Demulsifier chemical additives are commonly added to crude oil to enhance the separation of water-in-oil emulsions.¹⁵ Gradual accumulation of demulsifier molecules at the interface weakens the protective layer surrounding emulsified droplets. Once a sufficient concentration of demulsifier molecules at the interface is reached, water droplet flocculation and/or coalescence occurs upon contact.¹⁶ Previous studies reported a biodegradable polymer, ethyl cellulose (EC), effectively used as a demulsifier for water-in-diluted bitumen emulsions. Dosing emulsions with EC increased the flocculation-enhanced coalescence of water droplets through displacement of the protective interfacial layer.^{11,16,17}

Methods such as bottle tests and/or measurements of water content in oil (titration) are frequently used to determine the stability of emulsions. However, a much deeper understanding of emulsion stabilization mechanisms can be derived from studying the mechanical properties of the oil-water interfacial layer under compression and shear.¹⁸⁻²⁰ Shear rheology, a relatively new experimental technique,²⁰⁻²² is sensitive to layer growth and structural changes at the interface, whereas dilatational rheology highlights the interfacial coverage of surface active species and provides insights into dynamic changes of interfacial properties.¹⁸ However, a direct link between experimental results and emulsion stability of “real” process systems, where emulsified droplets collide randomly due to Brownian motion or under imposed shear, is often difficult to establish.

Although droplet coalescence promotes the oil-water phase separation, it is often inhibited by the presence of asphaltenes at the oil-water interface. These adsorbed species influence the surface forces acting between neighboring droplets and affect emulsion stability by controlling the drainage rate and collapse of the thin liquid film separating two droplets.²³ Measuring the

interaction forces as the oil-water interface deforms due to the close proximity of neighboring droplets is fundamental to understanding emulsion stabilization mechanisms.

Atomic force microscopy (AFM) has been previously utilized to investigate forces between solid surfaces (clean or coated). The technique has also been used to study deformations of oil-water and air-water interfaces and to measure surface forces between droplets or gas bubbles in aqueous systems.²⁴ Measurement of forces between a probe and rigid substrate using AFM has been well documented, and the separation between the colloidal probe and rigid substrate is determined using the slope of constant compliance region, where the force (F) depends linearly on piezo displacement. For systems involving a deformable interface, zero separation distance becomes more difficult to determine due to the coupling effect of interfacial deformation and cantilever bending upon applied force.²⁵⁻³⁰

Adsorbed interfacial species can greatly influence interaction forces and also govern the degree of droplet deformation under applied load, with the latter greatly influenced by interfacial rigidity.³¹ In the absence of hydrodynamic effects, droplet deformation results from the interaction forces exceeding the Laplace pressure.^{29,32} When droplets are pushed together, instead of reducing the separation distance between the droplet interfaces, as in the case of rigid substrates, the droplets flatten to increase their effective interaction area, with the distance unchanged when the disjoining pressure of the film between the droplets equals the Laplace pressure.³³

A theoretical approach has been developed to calculate the forces and deformations for particle-droplet, particle-bubble, droplet-droplet and bubble-bubble systems by applying the augmented Stokes-Reynolds-Young-Laplace (SRYL) equations.^{29,35} Droplet deformation can be well predicted for viscous interfaces where droplet shape is described by the Young-Laplace

equation.^{29,32,35-40} However, there is limited research which considers industrially relevant systems, such as water droplets in oil,⁴² or interfaces with significant elasticity, for which the criterion of a Laplacian response no longer holds.⁴³ Our previous study⁴⁴ explored viscoelastic effects encountered in water-in-crude oil emulsion systems. Oil-water interfacial stiffening and “skin” formation was observed upon water droplet aging in asphaltene solution, leading to the gradual formation of a viscoelastic oil-water interface. Incorporating dilatational elasticity into the SRYL equations was shown to accurately describe the deformation of aged water droplets under applied load.

The current research measures the forces of interaction between a silica sphere ($D \approx 8 \mu\text{m}$) and water droplets ($D \approx 70 \mu\text{m}$) in asphaltene- and bitumen-in-toluene solutions. Interaction forces and droplet deformations were measured with AFM for aged interfaces, and following demulsifier (EC) addition. This approach allows tracking of droplet deformation and forces in-situ, moving away from bulk and planar studies to industrially-relevant coalescing systems, with interfaces exhibiting elasticity. The water-crude oil system provides a unique opportunity to study interfaces which are originally viscous-dominant (Laplacian) and develop elasticity over time (non-Laplacian), while demulsifier addition reverts the interfacial aging. Tracking of these properties with AFM allows one to estimate the effectiveness of various surface active species, and the forces required to create and break emulsions.

MATERIALS AND METHODS

Materials

Syncrude Canada Ltd. kindly provided the vacuum distillation feed bitumen. HPLC-grade toluene and n-heptane were purchased from Fisher Scientific (Canada). Deionized water with 18.2 M Ω ·cm resistivity was used in all experiments. Silicon wafers from NanoFab (University of

Alberta) were used as substrates. Tipless cantilevers for force measurements and silicon nitride cantilevers for imaging were purchased from Bruker Scientific (USA). Silica microspheres ($D \approx 8 \mu\text{m}$) were purchased from Duke Scientific (USA) and mounted on the cantilevers to form colloidal probes. Ethyl cellulose with an ethoxyl content of 48 % and viscosity of 4 cP (EC-4; CAS 9004-57-3) was purchased from Sigma Aldrich (Canada).

Asphaltene Precipitation and Solution Preparation

The asphaltene precipitation method has been reported in detail elsewhere.⁴⁵ Bitumen was diluted with toluene and centrifuged to remove fine solids. The solvent was then removed through evaporation and n-heptane was added to the solids-free bitumen at a ratio of 40:1 by weight; the mixture was subsequently agitated on a mechanical shaker for 2 hr. After the supernatant was removed from the n-heptane-bitumen mixture, fresh n-heptane was added to wash away entrained maltenes in the precipitated asphaltenes.⁴⁵ The centrifugation-maltenes removal process was repeated several times until the supernatant was clear.

Fresh asphaltene- and bitumen-in-toluene solutions were prepared for each experiment by dissolving the required amount of asphaltenes or bitumen in toluene, and sonicating the solution for 15 min in an ultrasonic bath. To compare the two systems, bitumen concentration was adjusted to produce an equivalent asphaltene concentration, i.e. 0.588 g/L bitumen-in-toluene equaled 0.1 g/L asphaltene-in-toluene. The amount of asphaltene in bitumen was determined using the standard asphaltene precipitation method previously described by Zhang et al.⁴⁵ Two additional asphaltene concentrations (0.05 and 0.2 g/L) were also considered in this study.

EC-4 stock solution of 1 g/L was prepared by adding the required amount of EC to toluene and sonicating the mixture for 15 min in an ultrasonic bath. The role of EC-4 as an effective demulsifier was assessed by dosing EC-4 at 0.13 g/L into asphaltene or bitumen solutions with

an immersed water droplet. The dosing concentration was based on previous findings which showed effective demulsification of water-in-oil emulsions at 130 ppm (0.13 g/L).¹⁶

Preparation of the Cantilevers and Substrates

Silica spheres ($D \approx 8 \mu\text{m}$) were glued onto the tip of the long wide-beam or short narrow-beam AFM cantilever (model NP-O10 (Bruker, USA)) using a two-component epoxy (EP2LV, Master Bound, USA). The cantilevers were then placed in a vacuum desiccator for 24 hr and subsequently exposed to UV for 1 hr. Cantilever spring constant values were $\sim 0.12 \text{ N/m}$ for the short narrow-beam and $\sim 0.22 \text{ N/m}$ for the long wide-beam probes. These values did not change significantly during force measurements ($< 10 \%$).

Silicon wafers used as underlying substrates for anchoring water droplets in oil, were exposed to piranha solution for 1 hr and then immersed in 1 mM octadecyltrichlorosilane-in-toluene solution (OTS; ACROS Organics, Belgium) for 30 s. They were then rinsed with toluene and dried with nitrogen, resulting in a contact angle of $45\text{-}50^\circ$ in air. When submerged in solvent, the water droplet contact angle increased to 84° in toluene and 86° in asphaltene- and bitumen-in-toluene solutions, as shown in the Supporting Information Figure S-1. The intermediate contact angle is highly desirable to ensure that the deposited water droplets remained spherical and anchored on the substrate during AFM force measurements, although higher contact angle could be achieved by increasing the OTS concentration in solvent and/or extending OTS treatment time.

For force measurements between two water droplets, the underlying substrate was treated with 1 mM OTS-in-toluene solution for 2 min, resulting in a contact angle of 86° in air and 150° in toluene. This resulted in weakly attached water droplets to the substrate in solution and enabled easy pick-up of the water droplets by the AFM cantilever for droplet-droplet measurements.

Measurement of Contact Angle and Interfacial Tension

Water droplet contact angles on the solid substrate in air and in solvent, as well as the interfacial tension for water/asphaltene solution and water/bitumen solution were measured using a Theta Optical Tensiometer T200 (Biolin Scientific, Stockholm, Sweden). The instrument camera was calibrated and fresh asphaltene/bitumen solutions prepared for each test.

Contact angle measurements on treated silicon wafers were conducted either in air or in asphaltene- and bitumen-in-toluene solutions. For measurements in air, a water droplet ($V \approx 9 \mu\text{L}$) was deposited on the substrate, with the profile brought into focus and was recorded for 3 min at 3 fps. The contact angle was determined using the Theta software. For measurements in solvent, the substrate was positioned in a quartz cell and a water droplet ($V \approx 9 \mu\text{L}$) was placed on the substrate before gently adding asphaltene or bitumen solution to the quartz cell. The contact angle in this case was recorded over 60 min to provide comparison with the AFM study.

For interfacial tension measurements a water droplet ($V \approx 6 \mu\text{L}$) was generated from a 1 mL Hamilton syringe with an 18 gauge needle (Reno, NV). Profiling of the water droplet in either asphaltene- or bitumen-in-toluene solution was captured at a rate of 3 fps or higher for 60 min and analyzed using the vendor supplied software. The contact angle was recorded to verify the stability of the water droplet on the substrate surface in asphaltene-in-toluene or toluene-diluted bitumen solutions during the colloidal force measurements.

Three measurements were conducted per test condition and the variation in the measured values was less than 10 %. To measure the effect of demulsifier the EC-4 stock solution was added to the quartz cell following the aging of a water droplet in asphaltene or bitumen solutions for 1 hr. The interfacial aging time and demulsifier concentration (0.13 g/L) were selected to be consistent with the AFM study.

Dilatational Elasticity Measurements

The dilatational viscoelastic complex modulus, E was measured with the pulsating droplet module (PD 200) of the Theta Optical Tensiometer T200. During these measurements, a water droplet with $V \approx 6 \mu\text{L}$ was formed at the tip of an 18-gauge needle in asphaltene and bitumen solutions and oscillated sinusoidally. The droplet area and interfacial tension changes were recorded over time to obtain the viscous and elastic moduli.^{19,46,47} The droplet volume change was set to 10% during the oscillation, with the oscillation frequency of 0.1 Hz. Each reported dilatational elasticity consisted of 10 oscillations with a 10 s delay between each subsequent measurement. Measurements were carried out in asphaltene-in or bitumen-in toluene solutions for 55 min, after which EC-4 was added to the system to a total demulsifier concentration of 0.13 g/L.

AFM Force Measurements

Forces of interaction between a silica sphere and water droplet was measured using the Agilent 5500 AFM, equipped with a sealed environmental chamber. Deflection sensitivity and spring constant values of the cantilevers against the substrate were calculated by the Thermal K function before and after force measurements.

Water (0.5 wt. %) was added to the various asphaltene and bitumen solutions and were sonicated for 5 s to form an emulsion which was then injected into the AFM liquid cell. The setpoint for the force measurements was set to 0 V, while the piezo displacement was set to 4 μm , with all of the measurements obtained room temperature (24 °C). To eliminate the effect of solvent evaporation and subsequent changes in asphaltene concentration, interfacial aging was limited to 1 hr.

In this study, the following AFM force measurements were conducted:

1. Probe-droplet interactions. For probe-droplet force measurements water droplets ($D \approx 60\text{-}80\ \mu\text{m}$) remained strongly anchored on a partially hydrophobized (86°) substrate in asphaltene or bitumen solutions. The water droplets were aged for 15 min before the $8\text{-}\mu\text{m}$ particle was aligned over the water droplet and approached at $1\ \mu\text{m/s}$. The 15-min aging time was selected to represent the typical residence time of water droplets in diluted bitumen, as encountered in crude oil processing. Following 1 hr aging, EC-4 stock solution was added to the AFM liquid cell (1 mL total volume) at a net EC concentration of $0.13\ \text{g/L}$. The first force profile following the addition of EC-4 was collected at 7 min due to the intricate experimental setup and cantilever approach time.

2. Droplet-droplet interactions. For the droplet-droplet measurements in asphaltene solution, the cantilever was first positioned above a fresh water droplet on the hydrophobized substrate (150°), and lowered into contact using the same setpoint voltage as for the case of particle-droplet interaction. For freshly prepared water droplets in asphaltene solution (aging time less than 5 min), the droplet readily spreads on the surface of the cantilever. This was achieved by holding the cantilever in contact with the droplet for 5 s before retracting the cantilever and removing the droplet from the underlying substrate. The droplet ($D \approx 70\ \mu\text{m}$) was subsequently used to measure droplet-droplet interactions in $0.1\ \text{g/L}$ asphaltene-in-toluene solution after 15 min aging. The cantilever approach and retract velocity was fixed at $1\ \mu\text{m/s}$.

RESULTS AND DISCUSSION

Force Interactions between Rigid and Deformable Interfaces

The geometrical configuration of adsorbed layers on solid surfaces is frequently extrapolated to explain interactions in the presence of surface active agents, as encountered in emulsion systems. However, direct comparisons between “model” planar surfaces and “real” emulsion interfaces

are difficult to make, since droplet curvature and deformation greatly affect the adsorption and displacement of surface-active species.³¹

For the crude oil system, AFM was used to compare the forces of interaction between asphaltenes adsorbed on solids and those at liquid interfaces (Figure 1). To ensure the development of a uniform asphaltene layer the surfaces/interfaces were allowed to age for 15 min.¹²

Case I: Force curves were collected at 15 min following the injection of 0.1 g/L asphaltene-in-toluene solution between the silica particle and planar substrate (i.e. two rigid surfaces). During approach and retraction, short-range steric repulsion and weak adhesion (0.5 nN), with a relatively abrupt pull-off was observed (Figure 1(a)). The occurrence of repulsion agrees with previously published research, where the swollen asphaltene structure of polyaromatic core and aliphatic branches led to steric hindrance in good solvent (toluene).^{48,49} Interpenetration of the aliphatic branches of asphaltenes leads to the observed adhesion between the two asphaltene layers. The slope of the constant compliance region is very high at 1457 mN/m (Table 1), as expected for interactions between rigid surfaces.

Case II: 0.1 g/L asphaltene-in-toluene solution was injected into the AFM liquid cell, and the forces between a silica particle ($D \approx 8 \mu\text{m}$) and a deformable oil-water interface (water droplet with $D \approx 80 \mu\text{m}$ pinned on the silica substrate) was measured after 15-min interfacial aging. During the approach (Figure 1(a)), the slope of the high force constant compliance region is much lower (28.9 mN/m) than that for the coated substrates (Case I), indicating a more deformable interface. During the retraction (Figure 1b), the net adhesion force between the two interacting surfaces is significantly greater than that between two rigid surfaces (2.4 nN versus 0.5 nN). The increase in adhesion likely results from an increase in the contact area between the

two interacting surfaces compounded by a softer oil-water interface, as the solid particle is partially engulfed by the deformable interface (see schematic in Figure 1). It should be noted that the colloidal silica probe did not break the oil-water interface, as otherwise the laser signal would be lost, should the film be ruptured.

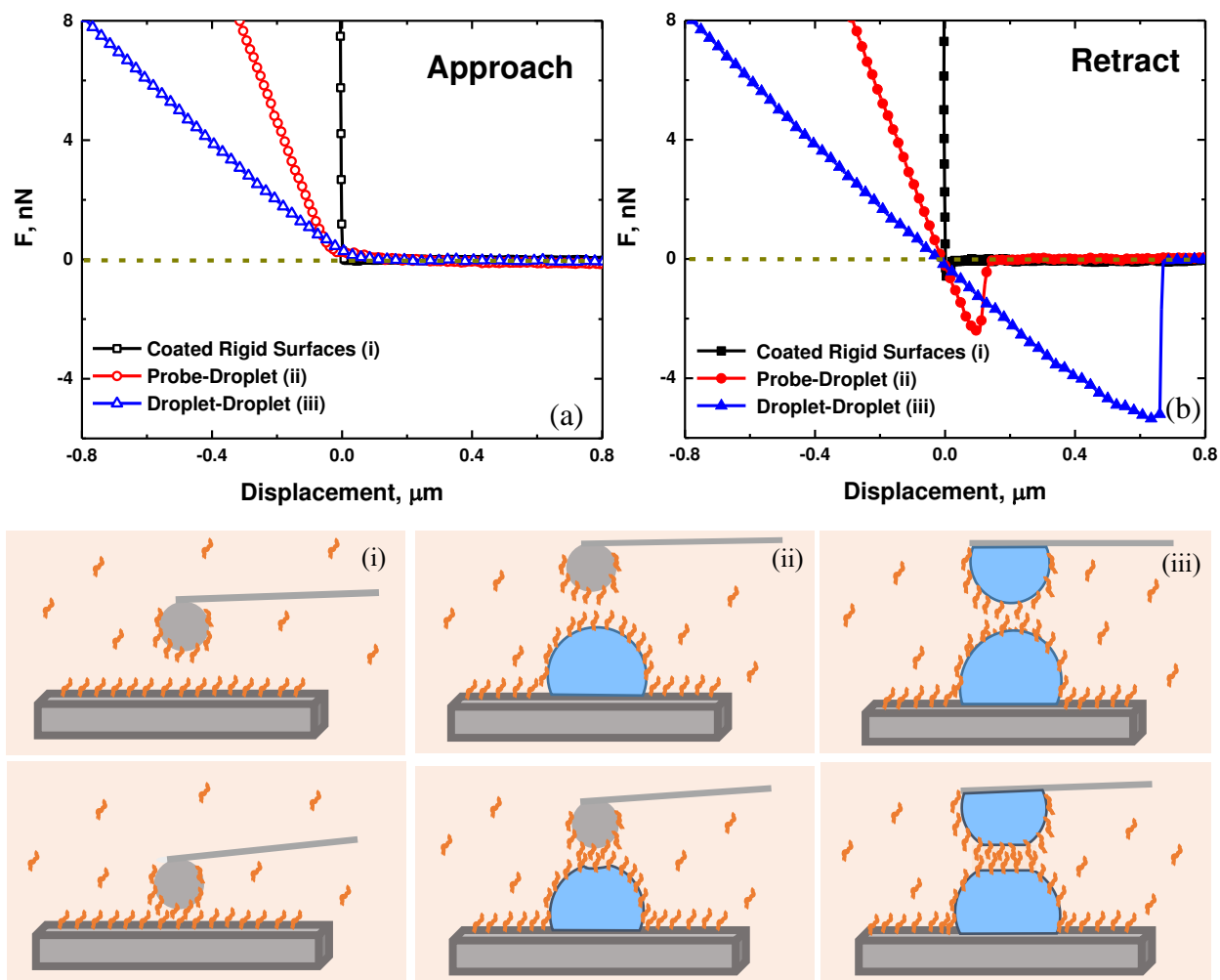


Figure 1. Interactions between various surfaces upon (a) approach (open symbols) and (b) retraction (filled symbols) after 15 min aging in 0.1 g/L asphaltene-in-toluene solution. Symbols: interactions between (i) coated rigid surfaces; (ii) a silica probe ($D \approx 8 \mu\text{m}$) and water droplet ($D \approx 80 \mu\text{m}$); (iii) two water droplets of similar size ($D \approx 70$ and $80 \mu\text{m}$). The schematic below the experimental data features the different systems far apart (top row) and in close proximity (bottom row), demonstrating the likely interfacial deformations.

Case III: 0.1 g/L asphaltene-in-toluene solution was injected into the AFM liquid cell prior to measuring the forces of interaction between two water droplets. The AFM cantilever with the attached water droplet ($D \approx 70 \mu\text{m}$) was centered over a second water droplet of similar size ($D \approx 80 \mu\text{m}$) and interaction forces were measured at 15 min aging. In this case, the slope of the high force constant compliance region was 10.6 mN/m; this reduced slope is once again attributed to increased deformation in the system (Figure 1(iii)). The presence of a second deformable droplet led to a further increase in the adhesion force on retraction (5.4 nN), likely from the increased local contact area and “flattening” of the interface as droplets are brought together. For the various systems considered in this study, it should be noted that the reported adhesion forces in Figure 1 (b) and Table 1 represent the total adhesion force, which is influenced by the properties of the interacting surfaces, i.e., contact area for deformable droplet-droplet \gg solid particle-substrate.

Table 1. The adhesion force (F_{ad}) and slope of the constant compliance region (k) from Figure 1.

	k (mN/m)	F_{ad} (nN)
Coated Rigid Surfaces in Asphaltene Solution (i)	1457	0.5
Probe-Droplet in Asphaltene Solution (ii)	28.9	2.4
Droplet-Droplet in Asphaltene Solution (iii)	10.6	5.4

Adhesion forces in Asphaltene- and Bitumen-Stabilized Systems

A comparison between adhesion forces measured in asphaltene and bitumen solutions is shown in Table 2. Interaction forces were measured between a silica colloidal probe and water droplet at 15 min following the injection of the test solution. Asphaltene concentration was varied between 0.05 and 0.2 g/L, with the corresponding bitumen concentration equal to 0.284 and 1.117 g/L, respectively. Using AFM to study equivalent asphaltene concentrations in toluene and bitumen

allows us to directly compare in-situ the forces acting between interfaces stabilized by asphaltenes and other interfacially active components in bitumen, such as resins and naphthenic acids.^{9,10}

Table 2. Adhesion force (F_{ad}) between a silica probe ($D \approx 8 \mu\text{m}$) and water droplet ($D \approx 70\text{-}80 \mu\text{m}$) in asphaltene and bitumen solutions of equivalent asphaltene concentrations after 15 min aging. Cantilever velocity = $1 \mu\text{m/s}$.

Asph. Conc. (g/L)	Adhesion Force F_{ad} (nN)	Bit. Conc. (g/L)	Adhesion Force F_{ad} (nN)
0.05	3.2 ± 0.6	0.284	3.8 ± 0.6
0.1	3.3 ± 0.6	0.588	3.6 ± 0.6
0.2	4.1 ± 0.8	1.117	4.7 ± 0.9

The force of adhesion between the silica particle and water droplet was shown to be in the range of 3.2 - 4.1 nN and 3.8 - 4.7 nN for asphaltene and bitumen solutions, respectively. While the increasing average adhesion force is mostly attributed to the changes in asphaltene concentration, it is worth noting that the average adhesion forces measured in bitumen solutions are consistently greater than those measured in asphaltene solutions. However, we acknowledge that the adhesion force magnitude for the asphaltene and corresponding bitumen cases is statistically within the experimental error. Although asphaltenes are expected to be the dominant interfacial component,^{6,7} the presence of other indigenous species in bitumen may contribute to the overall adhesion between the two interacting interfaces.⁵⁰

The “jump-in” adhesion force at the highest asphaltene concentration may be justified by the increased interpenetration of voluminous asphaltene layers. At high asphaltene concentrations,

previous research using surface forces apparatus (SFA) showed that the asphaltene layer thickness increases more rapidly, forming thick (multi-layer) interfacial layers which exhibit significant compressibility under normal force (i.e. soft, voluminous layers). Increased layer compressibility contributes to higher adhesion forces due to increased interpenetration and contact area between asphaltene layers.^{48,51}

The force measurements presented in the current study were conducted at a fixed slow cantilever velocity of 1 $\mu\text{m/s}$. At this low velocity the force during cantilever retraction represents a true measure of the adhesion force resulting from interpenetration of the adsorbed layers, as shown by jump-off during retraction. The effect of hydrodynamics on the force interaction is shown in the Supporting Information, Figure S-2, showing a hydrodynamic suction at velocities of 5 $\mu\text{m/s}$ or higher.

The Effect of Interfacial Aging and Demulsifier Addition

Water-oil interfaces have been shown to age as surface active species such as asphaltenes, fine particles, and surfactants partition at the liquid-liquid interface to form an interfacial layer in crude oil systems.^{4,8,20} The dominant interfacially active species in bitumen are asphaltenes, as inferred from Table 2 and from other studies.^{1-7,9,10} Asphaltene layers have been shown to exhibit time-dependent elasticity, similar to proteins and other surface active species,⁵² which with increased aging time result in a stable (solid-like) interfacial layer that can resist yielding.⁷ The rheological properties of the interfacial layer, more specifically the elastic modulus, has been shown to correlate to emulsion stability.⁵³

Our previous study demonstrated interfacial “stiffening” upon aging of a water droplet in asphaltene solution, and non-Laplacian behavior of the interface was highlighted by interfacial buckling upon droplet volume reduction.⁴⁴ The same phenomena of interfacial stiffening for a

water droplet in bitumen solution is shown in the inset of Figure 2. For 0.588 g/L bitumen-in-toluene the slope of the constant compliance region after 15 min aging is 32 mN/m and increases to 45 mN/m after 1 hr aging, comparable to the results for the asphaltene systems previously reported.⁴⁴ The increasing slope of constant compliance region in bitumen solution is also attributed to an increase in the interfacial dilatational elasticity (Figure 3(a)), since the change in water-bitumen interfacial tension, shown in Figure 3(b), between 15 and 60 min cannot adequately describe the measured changes in the slope of the constant compliance region.

To reduce the stiffness of the interfacial layer, amphiphilic demulsifier molecules are typically dosed at the ppm level in the organic phase to disrupt the interfacial network. The interaction forces between the silica probe ($D \approx 8 \mu\text{m}$) and water droplet ($D \approx 60 - 70 \mu\text{m}$) aged in 0.1 g/L asphaltene- and 0.588 g/L bitumen-in-toluene solutions for 1 hr and subsequently dosed with 0.13 g/L EC-4 are shown in Figure 2.

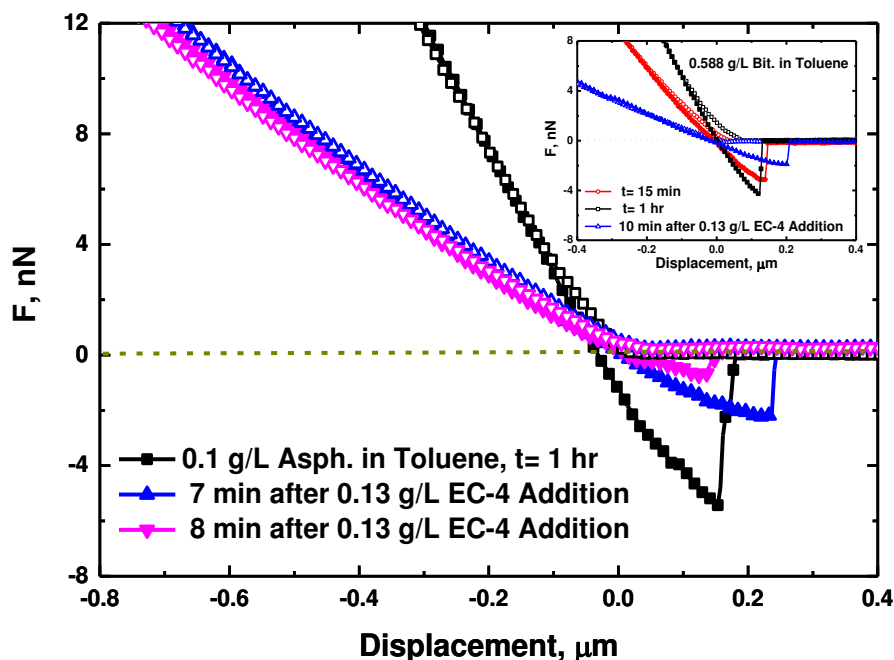


Figure 2. Forces of interaction between silica probe ($D \approx 8 \mu\text{m}$) and water droplet ($D \approx 60 - 70$

μm) in 0.1 g/L asphaltene-in-toluene at 1 hr aging and following the addition of 0.13 g/L EC-4. Cantilever approach and retraction force curves represented by the open and filled symbols, respectively. The cantilever velocity remained fixed at 1 $\mu\text{m/s}$. Inset: force profiles for a water droplet in 0.588 g/L bitumen-in-toluene solution ($D \approx 60 \mu\text{m}$) prior to and after EC-4 addition.

Firstly, considering the asphaltene system, the slope of the constant compliance region following 1 hr aging and in the absence of EC-4 is 41 mN/m, and the associated adhesion force between the particle and water droplet is 5.6 nN. Upon addition of EC-4, the slope of the constant compliance region and the particle-water droplet adhesion force continually decreases with demulsification time. Unfortunately, due to the complexity of the current measurement technique, we were unable to collect data within the first several minutes after demulsifier addition, as the demulsifier was added manually to the solution and the probe had to be re-aligned before it slowly approached the water droplet for the intended colloidal force measurements.

The time delay led to a significant reduction in the slope of constant compliance with $k = 18.5$ mN/m and 18.2 mN/m at 7 and 8 min demulsification time, respectively. While gradual softening of the interfacial layer is clearly measured at longer demulsification times, the significant reduction in the slope of constant compliance within the first 7 min indicates that the demulsification process is rather rapid. To study the competitive adsorption of EC-4 at the oil-water interface, the interfacial tension of a water droplet in asphaltene solution was measured, as shown in Figure 3(b). During the first hour of aging the interfacial tension reduced from 32 mN/m to 25 mN/m, confirming asphaltene adsorption, which has been shown to be a diffusion-limited process at short aging times.⁴⁸ At 1 hr interfacial aging, EC-4 was dosed to the asphaltene solution at a concentration of 0.13 g/L, and the interfacial tension was continuously measured.

The oil-water interfacial tension reduced to 12 mN/m in less than one minute, and further reduced by 2 mN/m in the next 15 min. The HLB of EC-4 is estimated to be 8, which is within the HLB range required for breaking water-in-oil emulsions.¹¹ The initial rapid reduction in interfacial tension following EC-4 addition confirms the competition of EC-4 molecules for available surface sites at the oil-water interface, followed by a slower secondary dynamic process which is most likely related to the relaxation/reorganization of the asphaltenes-EC composite film. This slower secondary dynamic process corresponds to the softening of the oil-water interface at longer demulsification times, as measured using the AFM technique (Figure 2).

It is worth noting that after 15 min demulsification time, the oil-water interfacial tension is almost equivalent to the equilibrium EC-4 only solution in toluene (IT = 9.5 mN/m), confirming significant displacement of the pre-formed asphaltene layer. While interfacial tension measurements are useful to study the competitive adsorption of surface active molecules, the reduction in oil-water interfacial tension alone is not always a suitable indicator for demulsification, and rather an approach to track the mechanical properties of the interfacial layer, for example using AFM, is favored. Overall, the AFM results show a reduction in the mechanical stiffness of the interfacial layer following the addition of EC-4 demulsifier. These findings are consistent with interfacial rheology measurements conducted at an asphaltene-stabilized planar oil-water interface, which report a diminished elasticity upon demulsifier addition.^{15,54} Similar findings are also observed with dilatational rheology (Figure 3(a)), where the elastic modulus of a droplet in asphaltene solution increases to 16 mN/m after ~1 hr aging and diminishes to 2 mN/m immediately following EC-4 addition.

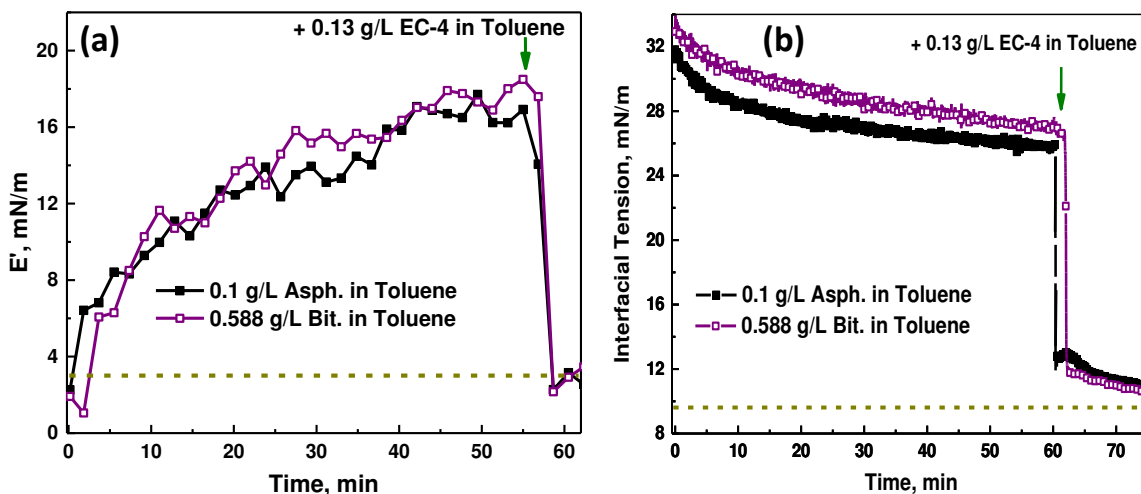


Figure 3. Time-dependent (a) dilatational elasticity and (b) interfacial tension (IT) of water droplets in 0.1 g/L asphaltene- and 0.588 g/L bitumen-in-toluene solutions. EC-4 was added as indicated by the arrows to a total demulsifier concentration of 0.13 g/L. The dashed lines represent the steady-state dilatational elasticity and IT values of a water droplet in 0.13 g/L EC-4-in-toluene solution.

A similar effect of interfacial layer softening was observed for the bitumen system. It is worth noting that the interfacial tensions for the asphaltene and bitumen systems almost overlap (likely indicating asphaltene to be the dominant interfacial component), and show a similar reduction in the interfacial tension following EC-4 addition (Figure 3(b)). Dilatational rheology (Figure 3(a)) also shows comparable data for asphaltene and bitumen systems as a droplet “stiffens” over time ($E' = 18$ mN/m after ~1 hr droplet aging). As EC-4 was dosed into the bitumen solution and the slope of constant compliance decreased from 45 mN/m to 17.9 mN/m (demulsification time = 10 min), the droplet elasticity also decreased to 2 mN/m (Figure 3(a)). The adhesion force between silica particle and water droplet was shown to reduce with increasing demulsification time. The reduction in adhesion force upon addition of EC confirms the rearrangement of the molecules at the interface and the likely formation of fractures in the network. Previous work confirmed EC’s

ability to flocculate water droplets at low concentrations. At high concentrations, however, EC addition promotes droplet coalescence, which would only occur upon rearrangement and/or “breaking” of the original stabilizing interfacial network.¹⁶ The main mechanism of demulsification using EC-4 has been shown to be droplet-droplet coalescence after its adsorption at the oil-water interface.^{11,54}

EC-4 has also been shown to reduce the thickness of the asphaltene/ bitumen interfacial film and irreversibly displace the asphaltenes/ bitumen from the interface.¹⁷ With the addition of EC-4, the interfacial properties of the stabilized water droplet, specifically the chemical composition of the interfacial layer (asphaltenes + EC-4 molecules), become adequately modified such that the silica probe was engulfed by the water droplet during cantilever approach. The critical demulsification time at which the silica particle would break the oil-water interface was 10 min and 12 min in asphaltene and bitumen solutions, respectively. Engulfment of the colloidal probe in the water droplet was easily identified by a loss of the laser signal. It is interesting to note that force measurements could not be conducted in EC-only solution and in “pure” toluene, as the probe was engulfed into the droplet immediately. Therefore, at the critical demulsification time for water in asphaltene-in-toluene or diluted bitumen emulsions, not only has the film softened significantly, but the uniform asphaltene/bitumen network has been sufficiently displaced, as shown in our earlier studies with AFM¹² and BAM.¹⁵ Such changes in the interfacial property lead to the observed particle immersion in the water droplet. With negligible electrical double layer force in organic solutions, the overall interaction force is attributed to the contributions from steric and van der Waals forces.

To ensure that the measured changes in the slope of constant compliance result from changes to the interfacial layer mechanical properties, the colloidal probe and water droplet were

individually assessed in the different solvent environments. Hydrophilic silica was exposed to asphaltene and bitumen solutions, and subsequently to EC-4, to represent changes to the surface properties of the colloidal probes. AFM topographical images of the substrates, given in the Supporting Information (Figure S-3 and Table S-1), show no significant change in aggregate height and roughness with increasing asphaltene/ bitumen concentration after demulsifier addition. Therefore, the changes in force and droplet deformation, as observed in Figure 2, are due to the changes in the structure and composition of the oil-water interfacial layer.

To further understand the mechanisms of droplet deformation, the high force SRYL model was applied to predict water droplet deformation in asphaltene solution upon aging and after demulsifier addition (Figure 4). The widely used high force SRYL equations with a pinned contact line boundary condition, developed for viscous Laplacian interfaces are given by:^{29,32,33}

$$\Delta D(y) \equiv \frac{F(t)}{4\pi\sigma} \left[\ln \left(\frac{F(t)R_{ds}}{8\pi\sigma R_0^2} \right) + 2B(\theta) - \frac{4\pi\sigma}{K} - 1 \right] \quad (1)$$

$$B(\theta) = 1 + \frac{1}{2} \ln \left[\frac{1+\cos(\theta)}{1-\cos(\theta)} \right] \quad (2)$$

$$R_{ds} \equiv \frac{1}{\left[\frac{1}{R_0} + \frac{1}{R_s} \right]} \quad (3)$$

where ΔD is the predicted displacement, $F(t)$ is the measured force, R_0 is the radius of the unperturbed droplet and R_s is that of the spherical probe; θ is the contact angle of the droplet on the substrate, σ is the interfacial tension, and K is the spring constant of the cantilever.

To predict the deformation of a water droplet, both the contact angle and oil-water interfacial tension should be known. The water droplet contact angle in asphaltene solution was measured to be 86° and remained independent of droplet aging, indicating a stable film of OTS anchored on the substrate as anticipated. However, the oil-water interfacial tension slowly decreased during asphaltene adsorption, and rapidly decreased following the addition of EC-4 (Figure

3(b)). It is worth highlighting a negligible change in the water droplet contact angle on the substrate following EC-4 addition, as shown in Figure S-1. The addition of EC however caused a significant reduction in $\gamma_{o/w}$ by 13 mN/m (see Figure 3(b)). Since the water droplet is first placed on the OTS treated substrate before solvent addition, it can be assumed that $\gamma_{w/s}$ remains fixed. Based on the well-established Young's equation, a decrease in $\gamma_{o/s}$ by 13 mN/m is anticipated to maintain the same ratio of $(\gamma_{o/s} - \gamma_{w/s})$ and $\gamma_{o/w}$, and hence the same contact angle. Our previous research on wettability modification of asphaltene-coated substrates by EC addition, showed an exponential decrease in the contact angle from $\sim 86^\circ$ to $\sim 61^\circ$ ($\Delta\theta = 25^\circ$ measured in air by water droplet) in 1 hr,¹² indicating an increase in $\gamma_{s/v}$ due to displacement of the preformed asphaltene layer by competitive adsorption of EC on the solid substrate. Such an increase in $\gamma_{s/v}$ led to the observed decrease in $\gamma_{o/s}$, and as discussed above, this competitive adsorption can counter-balance the reduction of $\gamma_{o/w}$ to maintain a constant contact angle θ following EC addition.

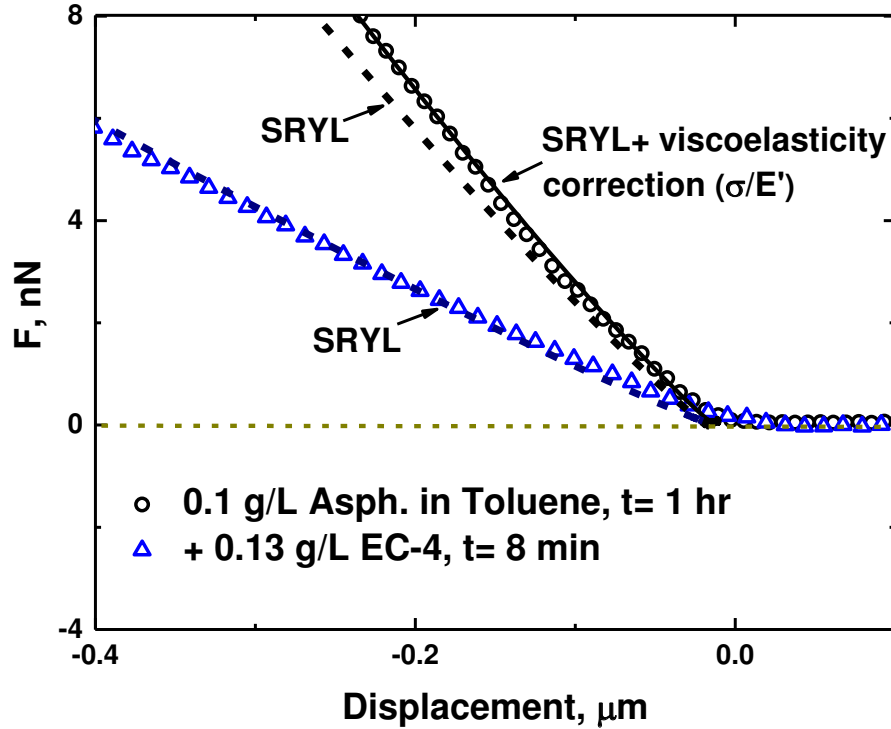


Figure 4. Measured forces (symbols) between a silica probe ($D \approx 8 \mu\text{m}$) and water droplet ($D \approx 70 \mu\text{m}$) in 0.1 g/L asphaltene-in-toluene solution and after EC-4 addition plotted against SRYL model predictions.

Using the appropriate measured values, Figure 4 shows the discrepancy between the experimental data and droplet deformation predicted by the SRYL equations for a water droplet aged for 1 hr in 0.1 g/L asphaltene-in-toluene solution. As shown in our previous study,⁴⁴ the change in interfacial tension upon droplet aging (Figure 3(b)) is not sufficient to explain the time-dependent “stiffening” of the oil-water interface. The elasticity of the oil-water interface, measured by dilatational rheology (Figure 3(a)) increased to 17 mN/m after ~1 hr aging, confirming the formation of a rigid asphaltene network.⁴⁴

To account for this high elasticity contribution, an experimentally measured viscoelasticity parameter (σ/E') is included as an extra term inside the brackets of Eqn. 1. Inclusion of the viscoelasticity parameter provides good agreement between experiment and theory when the

interfacial elasticity is a significant contribution to the overall interfacial stress. Interestingly, following the addition of EC-4, the modified SRYL model provides poor agreement to the experimental data. Due to the significant softening of the interfacial layer and a return to a Laplacian-like response, the dilatational elasticity is no longer a substantial component of the total interfacial stress (~ 2 mN/m) after EC-4 addition, as shown in Figure 3(a). As a result, the experimental data is best fitted using the SRYL equations, as shown in Figure 4. This behavior is consistent with a diminishing interfacial elasticity following demulsifier addition,¹⁵ which correlates with reduced emulsion stability.⁵⁴

CONCLUSIONS

This study considered the interaction forces between a silica probe and water droplet in asphaltene- and bitumen-in-toluene solutions. The net force observed in deformable systems was an order of magnitude higher than that for coated solid substrates. During the aging of water droplets in asphaltene and bitumen solutions, interfacial elasticity significantly contributed to the overall deformation of the water droplet under applied load and had to be incorporated into the high force Stokes-Reynolds-Young-Laplace equation. However, following the addition of EC-4, the slope of the constant compliance region confirmed a significant softening of the interfacial layer, and the mechanical response was similar to “fresh” water droplets in the asphaltene solution. Under this condition, the slope of the constant compliance region was suitably fitted using the SRYL equations. The results from this study highlight the application of AFM to study interactions in industrially relevant systems, where droplet deformation has a significant effect on emulsion stability, and multiple interfacially active species are present. Utilizing techniques that mimic the real systems (emulsions) provides an opportunity to better understand the micro-scale properties that govern the macro-scale behaviors.

AUTHOR INFORMATION

Corresponding Author

* Email: zhenghe.xu@ualberta.ca.

Notes

The authors declare no competing financial interest.

ACKNOWLEDGEMENTS

The authors are thankful for the financial support of this study by the Natural Sciences and Engineering Research Council (NSERC) Industrial Research Chair Program in Oil Sands Engineering and Alberta Innovates- Energy and Environmental Solutions (AI-EES).

REFERENCES

1. Masliyah, J.; Zhou, Z.; Xu, Z.; Czarnecki, J.; Hamza, H., Understanding water-based bitumen extraction from athabasca oil sands. *Can. J. Chem. Eng.* **2004**, 82 (4), 628-654.
2. Masliyah, J. H.; Xu, Z.; Czarnecki, J. A., - Handbook on Theory and Practice of Bitumen Recovery from Athabasca Oil Sands. - Kingsley Publishing Services, Cochrane (Canada), **2011**, vol.1.
3. Czarnecki, J. In Stabilization of water in crude oil emulsions. part 2, 2009; American Chemical Society: 1253-1257.
4. McLean, J. D.; Kilpatrick, P. K., Effects of Asphaltene Aggregation in Model Heptane–Toluene Mixtures on Stability of Water-in-Oil Emulsions. *J. Colloid Interface Sci.* **1997**, 196 (1), 23-34.
5. Tchoukov, P.; Czarnecki, J.; Dabros, T., Study of water-in-oil thin liquid films: Implications for the stability of petroleum emulsions. *Colloids Surf., A* **2010**, 372 (1-3), 15-21.
6. Czarnecki, J.; Tchoukov, P.; Dabros, T., Possible role of asphaltenes in the stabilization of water-in-crude oil emulsions. *Energy & Fuels* **2012**, 26 (9), 5782-5786.
7. Tchoukov, P.; Yang, F.; Xu, Z.; Dabros, T.; Czarnecki, J.; Sjoblom, J., Role of asphaltenes in stabilizing thin liquid emulsion films. *Langmuir* **2014**, 30 (11), 3024-3033.

8. Yarranton, H. W.; Sztukowski, D. M.; Urrutia, P., Effect of interfacial rheology on model emulsion coalescence. I. Interfacial rheology. *J. Colloid Interface Sci.* **2007**, 310 (1), 246-252.
9. Yan, Z.; Elliott, J. A. W.; Masliyah, J. H., Roles of Various Bitumen Components in the Stability of Water-in-Diluted-Bitumen Emulsions. *J. Colloid Interface Sci.* **1999**, 220 (2), 329-337.
10. Gao, S.; Moran, K.; Xu, Z.; Masliyah, J., Role of bitumen components in stabilizing water-in-diluted oil emulsions. *Energy & Fuels* **2009**, 23 (5), 2606-2612.
11. Feng, X.; Mussone, P.; Gao, S.; Wang, S.; Wu, S.-Y.; Masliyah, J. H.; Xu, Z., Mechanistic study on demulsification of water-in-diluted bitumen emulsions by ethylcellulose. *Langmuir* **2010**, 26 (5), 3050-3057.
12. Wang, S.; Segin, N.; Wang, K.; Masliyah, J. H.; Xu, Z., Wettability control mechanism of highly contaminated hydrophilic silica/alumina surfaces by ethyl cellulose. *J. Phys. Chem. C* **2011**, 115 (21), 10576-10587.
13. Angle, C. W.; Dabros, T.; Hamza, H. A., Demulsifier effectiveness in treating heavy oil emulsion in the presence of fine sands in the production fluids. *Energy & Fuels* **2007**, 21 (2), 912-919.
14. Hannisdal, A.; Ese, M.-H.; Hemmingsen, P. V.; Sjoblom, J., Particle-stabilized emulsions: Effect of heavy crude oil components pre-adsorbed onto stabilizing solids. *Colloids Surf., A* **2006**, 276 (1-3), 45-58.
15. Pensini, E.; Harbottle, D.; Yang, F.; Tchoukov, P.; Li, Z.; Kailey, I.; Behles, J.; Masliyah, J.; Xu, Z., Demulsification mechanism of asphaltene-stabilized water-in-oil emulsions by a polymeric ethylene oxide-propylene oxide demulsifier. *Energy & Fuels* **2014**, 28 (11), 6760-6771.
16. Feng, X.; Xu, Z.; Masliyah, J., Biodegradable polymer for demulsification of water-in-bitumen emulsions. *Energy & Fuels* **2009**, 23 (1), 451-456.
17. Hou, J.; Feng, X.; Masliyah, J.; Xu, Z., Understanding interfacial behavior of ethylcellulose at the water-diluted bitumen interface. *Energy & Fuels* **2012**, 26 (3), 1740-1745.
18. Erni, P., Deformation modes of complex fluid interfaces. *Soft Matter* **2011**, 7 (17), 7586-7600.

19. Miller, R.; Ferri, J. K.; Javadi, A.; Kragel, J.; Mucic, N.; Wustneck, R., Rheology of interfacial layers. *Colloid. Polym. Sci.* **2010**, 288 (9), 937-950.
20. Harbottle, D.; Chen, Q.; Moorthy, K.; Wang, L.; Xu, S.; Liu, Q.; Sjoblom, J.; Xu, Z., Problematic stabilizing films in petroleum emulsions: Shear rheological response of viscoelastic asphaltene films and the effect on drop coalescence. *Langmuir* **2014**, 30 (23), 6730-6738.
21. Spiecker, P. M.; Kilpatrick, P. K. Interfacial rheology of petroleum asphaltenes at the oil-water interface. *Langmuir* **2004**, 20 (10), 4022-4032.
22. Verruto, V. J.; Le, R. K.; Kilpatrick, P. K. Adsorption and Molecular Rearrangement of Amphoteric Species at Oil-Water Interfaces. *J. Phys. Chem. B* 2009, 113 (42), 13788-13799.
23. Gromer, A.; Penfold, R.; Gunning, A. P.; Kirby, A. R.; Morris, V. J., Molecular basis for the emulsifying properties of sugar beet pectin studied by atomic force microscopy and force spectroscopy. *Soft Matter* **2010**, 6 (16), 3957-3969.
24. Butt, H.-J.; Cappella, B.; Kappl, M., Force measurements with the atomic force microscope: Technique, interpretation and applications. *Surf. Sci. Rep.* **2005**, 59 (1-6), 1-152.
25. Bonaccorso, E.; Kappl, M.; Butt, H.-J. Thin liquid films studied by atomic force microscopy. *Curr. Opin. Colloid Interface Sci.* **2008**, 13 (3), 107-119.
26. Ducker, W. A.; Xu, Z.; Isrealachvili, J. N., Measurements of hydrophobic and DLVO forces in bubble-surface interactions in aqueous solutions. *Langmuir* **1994**, 10 (9), 3279-3289.
27. Hartley, P. G.; Grieser, F.; Mulvaney, P.; Stevens, G. W., Surface forces and deformation at the oil-water interface probed using AFM force measurement. *Langmuir* **1999**, 15 (21), 7282-7289.
28. Aston, D. E.; Berg, J. C., Quantitative analysis of fluid interface-atomic force microscopy. *J. Colloid Interface Sci.* **2001**, 235 (1), 162-169.
29. Chan, D. Y. C.; Klaseboer, E.; Manica, R., Film drainage and coalescence between deformable drops and bubbles. *Soft Matter* **2011**, 7 (6), 2235-2264.
30. Filip, D.; Uricanu, V. I.; Duits, M. H. G.; Van, D. E.; Mellema, J.; Agterof, W. G. M.; Mugele, F., Microrheology of aggregated emulsion droplet networks, studied with AFM-CSLM. *Langmuir* **2006**, 22 (2), 560-574.

31. Krasowska, M.; Prestidge, C. A.; Beattie, D. A., Atomic force microscopy for determining surface interactions of relevance for food foams and emulsions. In *Food Texture Design and Optimization*, John Wiley & Sons, Ltd: 2014; 402-422.
32. Tabor, R. F.; Chan, D. Y. C.; Grieser, F.; Dagastine, R. R., Structural forces in soft matter systems. *J. Phys. Chem. Lett.* **2011**, 2 (5), 434-437.
33. Tabor, R. F.; Grieser, F.; Dagastine, R. R.; Chan, D. Y. C., Measurement and analysis of forces in bubble and droplet systems using AFM. *J. Colloid Interface Sci.* **2012**, 371 (1), 1-14.
34. Uricanu, V. I.; Duits, M. H. G.; Filip, D.; Nelissen, R. M. F.; Agterof, W. G. M., Surfactant-mediated water transport at gelatin gel/oil interfaces. *J. Colloid Interface Sci.* **2006**, 298 (2), 920-934.
35. Chan, D. Y. C.; Dagastine, R. R.; White, L. R., Forces between a rigid probe particle and a liquid interface. I. The repulsive case. *J. Colloid Interface Sci.* **2001**, 236 (1), 141-154.
36. Webber, G. B.; Edwards, S. A.; Stevens, G. W.; Grieser, F.; Dagastine, R. R.; Chan, D. Y. C., Measurements of dynamic forces between drops with the AFM: Novel considerations in comparisons between experiment and theory. *Soft Matter* **2008**, 4 (6), 1270-1278.
37. Lockie, H.; Manica, R.; Tabor, R. F.; Stevens, G. W.; Grieser, F.; Chan, D. Y. C.; Dagastine, R. R., Anomalous pull-off forces between surfactant-free emulsion drops in different aqueous electrolytes. *Langmuir* **2012**, 28 (9), 4259-4266.
38. Manor, O.; Chau, T. T.; Stevens, G. W.; Chan, D. Y. C.; Grieser, F.; Dagastine, R. R., Polymeric stabilized emulsions: Steric effects and deformation in soft systems. *Langmuir* **2012**, 28 (10), 4599-4604.
39. Tabor, R. F.; Lockie, H.; Mair, D.; Manica, R.; Chan, D. Y. C.; Grieser, F.; Dagastine, R. R., Combined AFM-confocal microscopy of oil droplets: Absolute separations and forces in nanofilms. *J. Phys. Chem. Lett.* **2011**, 2 (9), 961-965.
40. Dagastine, R. R.; Manica, R.; Carnie, S. L.; Chan, D. Y. C.; Stevens, G. W.; Grieser, F., Dynamic forces between two deformable oil droplets in water. *Science* **2006**, 313 (5784), 210-213.
41. Shi, C.; Zhang, L.; Xie, L.; Lu, X.; Liu, Q.; Mantilla, C. A.; Van Den Berg, F. G. A.; Zeng, H., Interaction Mechanism of Oil-in-Water Emulsions with Asphaltenes Determined Using Droplet Probe AFM. *Langmuir* **2016**, 32 (10), 2302-2310.

42. Vakarelski, I. U.; Li, E. Q.; Thoroddsen, S. T., Soft colloidal probes for AFM force measurements between water droplets in oil. *Colloids Surf., A* **2014**, 462, 259-263.
43. Woodward, N. C.; Gunning, A. P.; Maldonado-Valderrama, J.; Wilde, P. J.; Morris, V. J., Probing the in Situ Competitive Displacement of Protein by Nonionic Surfactant Using Atomic Force Microscopy. *Langmuir* **2010**, 26 (15), 12560-12566.
44. Kuznicki, N. P.; Harbottle, D.; Masliyah, J. H.; Xu, Z. Dynamic Interactions between a Silica Sphere and Deformable Interfaces in Organic Solvents Studied by Atomic Force Microscopy. *Langmuir* **2016**, 32, 9797-9806.
45. Zhang, L. Y.; Lawrence, S.; Xu, Z.; Masliyah, J. H., Studies of Athabasca asphaltene Langmuir films at air-water interface. *J. Colloid Interface Sci.* **2003**, 264 (1), 128-140.
46. Liggieri, L.; Santini, E.; Guzmán, E.; Maestro, A.; Ravera, F., Wide-frequency dilational rheology investigation of mixed silica nanoparticle–CTAB interfacial layers. *Soft Matter* **2011**, 7, 7699-7709.
47. Ravera, F.; Loglio, G.; Kovalchuk, V. I. Interfacial dilational rheology by oscillating bubble/drop methods. *Curr. Opin. Colloid Interface Sci.* **2010**, 15 (4), 217–228.
48. Natarajan, A.; Kuznicki, N.; Harbottle, D.; Masliyah, J.; Zeng, H.; Xu, Z., Understanding mechanisms of asphaltene adsorption from organic solvent on mica. *Langmuir* **2014**, 30 (31), 9370-9377.
49. Wang, S.; Liu, J.; Zhang, L.; Masliyah, J.; Xu, Z., Interaction forces between asphaltene surfaces in organic solvents. *Langmuir* **2010**, 26 (1), 183-190.
50. Wu, X. Investigating the Stability Mechanism of Water-in-Diluted Bitumen Emulsions through Isolation and Characterization of the Stabilizing Materials at the Interface. *Energy & Fuels* **2003**, 17 (1), 179-190.
51. Natarajan, A.; Xie, X.; Wang, S.; Liu, Q.; Masliyah, J.; Zeng, H.; Xu, Z. Understanding Molecular Interactions of Asphaltenes in Organic Solvents Using a Surface Force Apparatus. *J. Phys. Chem. C* **2011**, 115, 16043-16051.
52. Bos, M. A.; Van Vliet, T., Interfacial rheological properties of adsorbed protein layers and surfactants: A review. *Adv. Colloid Interface Sci.* **2001**, 91 (3), 437-471.

- 53.** Georgieva, D.; Schmitt, V.; Leal-Calderon, F.; Langevin, D., On the possible role of surface elasticity in emulsion stability. *Langmuir* **2009**, *25* (10), 5565-5573.
- 54.** Harbottle, D.; Liang, Y.; Xu, Z. Asphaltene-stabilized emulsions: an interfacial rheology study. Paper presented at IBEREO 2015: Challenges in rheology and product development September 9-11, **2015**, Coimbra, Portugal.